

# Reversible Switching between Molecular and Charge Transfer Phases in a Liquid Crystalline Organic Semiconductor

Brian A. Gregg\* and Muhammet Erkan Kose\*

National Renewable Energy Laboratory, 1617 Cole Boulevard, Golden, Colorado 80401

Received March 31, 2008. Revised Manuscript Received June 10, 2008

We report the first experimental example, to our knowledge, of reversible switching between a molecular and a charge transfer phase in an organic semiconductor. An oriented film of liquid crystal perylene diimide molecules reversibly switches between a red phase with narrow conduction and valence bands and a large bandwidth black phase as the  $\pi$ -stacked chromophores shift just 1.6 Å relative to their neighbors. This shift causes a substantial change in the intermolecular electronic overlap between molecules. The polarization of maximum absorbance rotates  $\sim 90^\circ$ , from an apparently molecule centered transition to an intermolecular charge transfer (CT) transition polarized along the  $\pi$ - $\pi$  stacking axis. The experimental results are further explored via density functional theory calculations on a dimer model that demonstrate the variations in energy and oscillator strength of the molecular (Frenkel) and CT transitions as the longitudinal molecular offset is varied. These results demonstrate the exquisite sensitivity of the electrical properties of organic semiconductors to slight variations in molecular stacking.

## Introduction

Electronic interactions among planar  $\pi$ -stacked organic semiconductors are a topic of both fundamental and commercial interest. Quantum mechanical overlap between the  $\pi$ -orbitals of molecules in a quasi-one-dimensional stack is strongly dependent on geometrical factors. The magnitude of the in-phase overlap (electronic coupling), rather than the areal overlap, determines the strength of the intermolecular interactions and thereby the width of the conduction and valence bands and the color of the solid. Some crystal phases of perylene diimides<sup>1</sup> and phthalocyanines exhibit a strong long wavelength charge transfer (CT) band in the absorption spectrum, and the appearance of such CT bands seems to be a requirement for high photoconductivity.<sup>2,3</sup> The electrophotography industry, therefore, employs the CT phases of perylene diimides and phthalocyanines as the photoactive element in photocopiers and laser printers.<sup>4</sup> Despite their widespread use, a clear theoretical understanding of such CT materials is still lacking. We describe here an oriented phase of a liquid crystal perylene diimide that switches reversibly between a weakly coupled molecular-like phase and a strongly coupled CT phase after a shift of only  $\sim 1.6$  Å in molecular offset.

Besides their use in photocopiers, perylene diimides are also commercially important pigments (e.g., in automobile

paints) and more recently have been employed in organic solar cells, light emitting diodes, and field effect transistors.<sup>2,5–7</sup>

All derivatives show the same absorption spectrum in solution yet exhibit striking changes in color in the solid state depending on the side chains attached to the imide nitrogen. Crystal structure determinations show that these colors result from very slight changes in crystal packing.<sup>1,8</sup> Kazmaier and Hoffmann employed Hückel theory to investigate this “crystallochromy” and explained the changes as being caused by quantum interference effects: as the molecules in the stacks translate relative to their neighbors, the  $\pi$ -orbitals of the LUMO and HOMO move in and out of phase with each other leading to oscillations in conduction and valence bandwidths and therefore color.<sup>9</sup>

Frenkel excitons in these solids originate from molecular optical transitions and are necessarily polarized in the molecular plane, yet CT excitons have a polarization component along the  $\pi$ - $\pi$  stacking axis, as discussed by Hoffmann et al.<sup>10</sup> This group further showed by polarized absorption measurements on a weakly oriented perylene

\* Corresponding authors. E-mail: brian\_gregg@nrel.gov, muhammet\_kose@nrel.gov.

- (1) Klebe, G.; Graser, F.; Hädicke, E.; Berndt, J. *Acta Crystallogr., Sect. B* **1989**, *45*, 69.
- (2) Law, K.-Y. *Chem. Rev.* **1993**, *93*, 449.
- (3) Saito, T.; Sisk, W.; Kobayashi, T.; Suzuki, S.; Iwayanagi, T. *J. Phys. Chem.* **1993**, *97*, 8026. (a) Sims, T. D.; Pemberton, J. E.; Lee, P.; Armstrong, N. R. *Chem. Mater.* **1989**, *1*, 26.
- (4) Borsengerger, P. M.; Weiss, D. S. *Organic Photoreceptors for Imaging Systems*; CRC Press: New York, 1993; p 447. Diamond, A. S.; Weiss, D. S. *Handbook of Imaging Materials*; CRC Press: New York, 2002; p 676.

- (5) Gregg, B. A. *J. Phys. Chem. B* **2003**, *107*, 4688. Chen, S.-G.; Stradins, P.; Gregg, B. A. *J. Phys. Chem. B* **2005**, *109*, 13451. Jenekhe, S. E.; *Chem. Mater.* **2004**, *16* (23). Chesterfield, R. J.; McKeen, J. C.; Newman, C. R.; Ewbank, P. C.; daSilvaFilho, D. A.; Bredas, J.-L.; Miller, L. L.; Mann, K. R.; Frisbie, C. D. *J. Phys. Chem. B* **2004**, *108*, 19281. Organic- Based Photovoltaics. *MRS Bull.* **2005**, *30* (1). Forrest, S. R. *Chem. Rev.* **1997**, *97*, 1793. Peumans, P.; Yakimov, A.; Forrest, S. R. *J. Appl. Phys.* **2003**, *93* (7), 3693. Wöhrlé, D.; Meissner, D. *Adv. Mater.* **1991**, *3*, 129. Popovic, Z. D.; Hor, A.-M.; Loutfy, R. O. *Chem. Phys.* **1988**, *127*, 451. Popovic, Z. D.; Loutfy, R. O.; Hor, A.-M. *Can. J. Chem.* **1985**, *63*, 134.
- (6) Perlstein, J. *Chem. Mater.* **1994**, *6*, 319.
- (7) Pope, M.; Swenberg, C. E. *Electronic Processes in Organic Crystals and Polymers*, 2nd ed.; Oxford University Press: New York, 1999.
- (8) Graser, F.; Hädicke, E. *Liebigs Ann. Chem.* **1980**, 1994. Hädicke, E.; Graser, F. *Acta Crystallogr., Sect. C* **1986**, *42*, 189. Hädicke, E.; Graser, F. *Acta Crystallogr., Sect. C* **1986**, *42*, 195.
- (9) Kazmaier, P. M.; Hoffmann, R. *J. Am. Chem. Soc.* **1994**, *116*, 9684.
- (10) Hoffmann, M.; Schmidt, K.; Fritz, T.; Hasche, T.; Agranovich, V. M.; Leo, K. *Chem. Phys.* **2000**, *258*, 73.

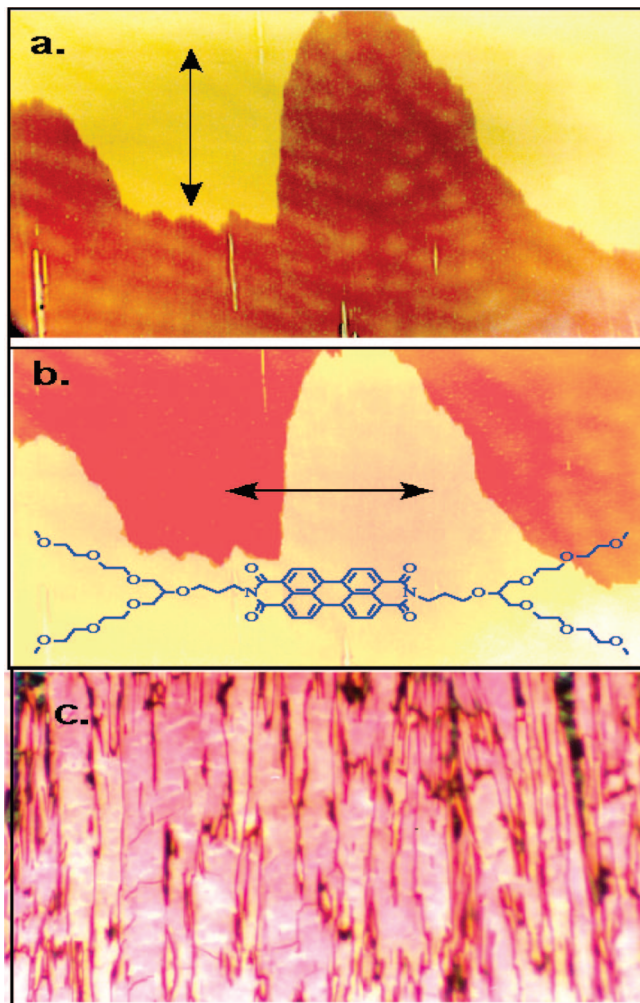


**Figure 1.** a and b. Photomicrographs taken with polarized light of the same 1.2 mm wide spot on a rub-aligned film of PPMEEM (structure shown in inset of b) at the phase boundary between the encroaching black phase and the receding red phase. a. Polarizer (indicated by arrow) oriented along the rubbing direction. b. Polarizer perpendicular. c. 0.3 mm wide view of the aligned crystallites imaged between crossed polarizers. This structure does not change during the red to black phase transition.

diimide film that the lower energy optical transitions did, in fact, exhibit some intermolecular character, thus confirming the existence of CT excitons.

### Experimental Section

The synthesis and chemical characterization of the liquid crystalline perylene diimide PPMEEM (structure shown in inset to Figure 1b) has been described previously.<sup>11</sup> This compound is a liquid crystal at room temperature with a clearing (liquid crystal to isotropic) point of 55 °C. When prepared as a thin film on many substrates, it spontaneously organizes into a layered structure with the  $\pi$ - $\pi$  stacking axis of the molecules aligning parallel to the substrate.<sup>11</sup> In this work, thin films (~50 nm) of PPMEEM are spin-coated from THF solution onto glass slides rubbed with poly(tetrafluoroethylene) as an alignment layer. The films grow in highly oriented polycrystalline domains with the long crystal axes of the 10–40  $\mu\text{m}$  wide crystallites oriented along the rubbing direction (Figure 1c). Once the oriented, thermodynamically stable black phase has crystallized, and it may be transformed within

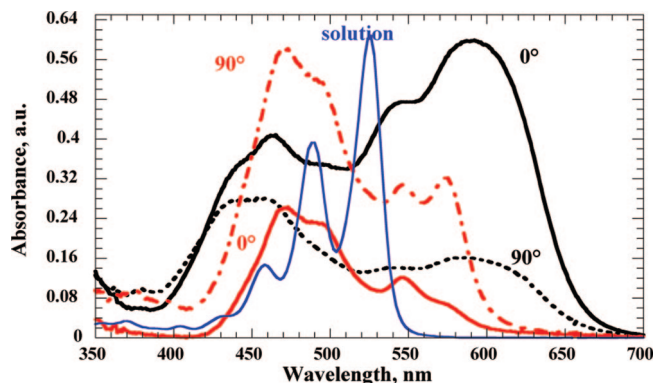


**Figure 2.** Polarized absorption spectra for the red phase (labeled on left), the black phase (labeled on right), and the chloroform solution spectrum (middle).

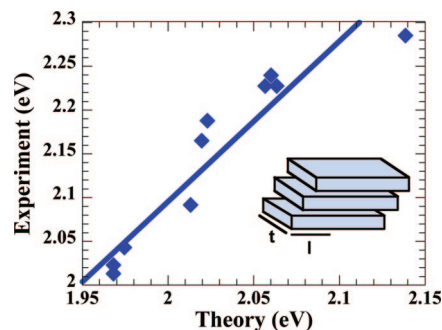


**Figure 3.** Comparison of calculated and experimental excited-state energies of several substituted perylene diimides. Experimental data were taken from ref 1. Inset shows the  $\pi$ - $\pi$  stacking motif of the PPMEEM molecules and indicates the transverse and longitudinal,  $t$  and  $l$ , offset directions.

seconds into the red phase by exposure to warm water vapor at ~40 °C. This does not change the observed crystallite structure; however, the film does swell, presumably incorporating water molecules. Left under ambient laboratory conditions, the black phase grows back spontaneously after 10–20 h.

Photomicrographs of the oriented films were obtained on a Nikon Labphot 2 polarizing microscope with a Nikon FX-35DX camera, while polarized absorption spectra were obtained with an HP 8453 spectrophotometer fitted with a film polarizer and a calibrated rotating sample holder.

### Results and Discussion

**Molecular  $\pi$ -Stacks.** Perylene diimides exhibit an almost universal quasi-1-D stacking motif: the aromatic rings align parallel to each other at a distance near 3.4 Å.<sup>1,6</sup> Each molecule is related to its nearest neighbors via translation along the transverse and longitudinal directions (referenced to the molecular core, see inset to Figure 3). Different side chains attached to the imide nitrogen result in different transverse,  $t$ , and longitudinal,  $l$ , offsets, causing a change in the tilt angle of the long molecular axis with respect to the  $\pi$ - $\pi$  stacking axis.<sup>6</sup> The tilt angles of the aromatic planes in the red and black films of PPMEEM were determined by XRD measurements<sup>12</sup> to be 62.0° and 45.6° relative to the substrate plane, respectively. It was not possible to distinguish between  $t$  and  $l$ ; however, it was determined that the total

(11) Cormier, R. A.; Gregg, B. A. *J. Phys. Chem. B* **1997**, *101*, 11004. (a) Cormier, R. A.; Gregg, B. A. *Chem. Mater.* **1998**, *10* (5), 1309.

(12) Liu, S.-G.; Sui, G.; Cormier, R. A.; Leblanc, R. M.; Gregg, B. A. *J. Phys. Chem. B* **2002**, *106*, 1307.

displacement  $(l^2 + l'^2)^{1/2} = 1.57 \text{ \AA}$ . Thus, the molecules shift  $\sim 1.6 \text{ \AA}$  relative to their neighbors in the stack. Kazmaier and Hoffmann calculated that the repeat distance between nodes in the HOMO in the longitudinal offset direction is  $4.5 \text{ \AA}$ , while in the LUMO, having one more node, it is  $2.7 \text{ \AA}$ .<sup>9</sup> The measured shift of PPMEEM molecules between phases is approximately half these lengths, about the difference from peak to valley; thus, this small change may be expected to cause major perturbations in optoelectronic properties.

**Polarized Absorption Spectra.** Figure 1a,b shows two polarized optical micrographs of the same spot on an oriented PPMEEM thin film taken at the phase boundary between the encroaching black phase and the receding red phase. The long-range ordering ( $>1 \text{ cm}^2$ ) of these films and the fact that the phase change does not alter the orientation of the crystallites (Figure 1c) provides an opportunity to study the opto-electronic effects of subtle morphological changes between the  $\pi$ -stacked molecules. When incident light is polarized along the rubbing direction, denoted  $0^\circ$  (Figures 1a and 2), the black phase has its maximum optical absorption while the red phase shows its minimum absorption. The opposite result is observed with perpendicularly ( $90^\circ$ ) polarized light (Figures 1b and 2). Thus the polarization of maximum absorbance rotates  $\sim 90^\circ$  during the phase transition. However, the crystals (Figure 1c) appear to be twinned; thus, some angular components of the transition dipole may be averaged out when measuring over multiple crystals as in our experiments. Thus the transition dipole in a single crystallite may rotate less than  $90^\circ$  between the two phases. The  $\pi$ -stacked molecules are tilted closer to horizontal than vertical when imaged from above; thus, the  $90^\circ$  polarized light probes mainly the long molecular axis, while the  $0^\circ$  light is polarized approximately along the  $\pi$ - $\pi$  stacking axis (the long crystal axis).<sup>12</sup>

The maximum red phase absorption occurs at  $0.27 \text{ eV}$  higher energy than the molecular absorption in solution ( $2.36 \text{ eV}$ ), suggesting that the optical transition is destabilized by interaction with neighboring molecules. The absorption intensity decreases with an almost unchanged spectrum from  $90^\circ$  to  $0^\circ$  (Figure 2), with the exception of the longest wavelength band at  $574 \text{ nm}$  that almost vanishes at  $0^\circ$ . The polarization ratio is constant across most of the spectrum showing that this absorption is primarily from a single transition which we assign to the molecule centered (Frenkel) transition. The small peak at  $574 \text{ nm}$  is assigned to a weak CT band. The maximum absorption of the black phase, on the other hand, occurs  $0.27 \text{ eV}$  lower than the molecular absorption in solution indicating that the optical transition is now stabilized by interaction with neighboring molecules. The absorption intensity decreases much more rapidly at the long wavelength peak ( $593 \text{ nm}$ ) than at the short wavelength peak ( $462 \text{ nm}$ ) as the polarizer is rotated from  $0^\circ$  to  $90^\circ$ . This change in polarization ratio indicates that the short wavelength transition has a different origin than the longer wavelength transition—these are assigned to the molecule centered and CT transitions, respectively. The energy of the  $(0, 0)$  band, a proxy for the semiconductor optical bandgap, decreases from  $2.11 \text{ eV}$  in the red phase to  $1.95 \text{ eV}$  in the

black phase.<sup>12</sup> This suggests that the sum of the valence and conduction bandwidths increases by  $\sim 320 \text{ meV}$  during this reversible transition,<sup>9</sup> a very large change for an organic semiconductor.

These results might be explained by molecular exciton theory of  $\pi$ -stacked molecules with parallel transition dipoles.<sup>7,13</sup> However, in contrast to the predictions of this model, both high and low energy transitions are optically allowed in both phases, and the absorption spectra of perylene diimides are independent of the number of molecules in their unit cells.<sup>1,12</sup> The quantum interference model is suggestive and may be qualitatively correct,<sup>9</sup> but Hückel theory cannot treat intermolecular CT transitions. More recent theories of optical and electro-optical transitions in similar materials often employ PTCDA (perylene tetracarboxylic dianhydride, the parent compound of perylene diimides) as the model compound. Transitions are treated as linear combinations of localized Frenkel and CT excitons coupled to a high frequency internal vibration.<sup>10,14</sup> Unfortunately, PTCDA does not exhibit the strong, long wavelength CT band required for high photoconductivity. Some theoretical treatments of more strongly coupled CT materials have appeared recently,<sup>15</sup> but this remains an area of active research.

In an attempt to semiquantitatively explore the nature of these optical transitions, we employ time-dependent density functional theory (TD-DFT) calculations. The excited-state energies and oscillator strengths of a perylene diimide dimer model are calculated as a function of the longitudinal offset between molecules. Although TD-DFT is known to underestimate the energies of CT transitions, we find reasonable agreement with our experimental results. Due to the local nature of the approximate exchange correlation functional, TD-DFT calculations for long-range charge transfer excitations have been reported to result in lower values as large as  $1 \text{ eV}$  or more.<sup>16</sup> On the other hand in a number of calculations on dimeric systems where there is a strong orbital overlap between the frontier orbitals of the molecules, the underestimation of TD-DFT decreases to  $0.1$ – $0.2 \text{ eV}$  for charge-transfer transitions.<sup>17</sup> Magyar and Tretiak examined the effect of orbital exchange on the calculation of charge transfer states in various interacting chromophores. From their results, they concluded that TD-DFT might be used to calculate charge transfer transitions of strongly coupled systems by using hybrid functionals with a small amount of orbital exchange.<sup>18</sup>

**Excited-State Calculations on Perylene Diimides.** Since there is a negligible contribution of alkyl-substituted side

(13) Kasha, M.; Rawls, H. R.; El-Bayoumi, A. *Pure Appl. Chem.* **1965**, *11*, 371.

(14) Hennessy, M. H.; Soos, Z. G.; Pascal, R. A., Jr.; Girlando, A. *Chem. Phys.* **1999**, *245*, 199. (a) Mazur, G.; Petelenz, P.; Slawik, M. *J. Chem. Phys.* **2003**, *118* (3), 1423. Vragovic, I.; Scholz, R. *Phys. Rev. B* **2003**, *68*, 155202.

(15) Nakai, K.; Ishii, K.; Kobayashi, N.; Yonehara, H.; Pac, C. *J. Phys. Chem. B* **2003**, *107*, 9749. Schuster, R.; Knupfer, M.; Berger, H. *Phys. Rev. Lett.* **2007**, *98*, 037402.

(16) Dreuw, A.; Head-Gordon, M. *J. Am. Chem. Soc.* **2004**, *126*, 4007.

(17) Nunzi, F.; Fantacci, S.; DeAngelis, F. *J. Phys. Chem. C* **2008**, *112*, 1213. Raon, J. G. S. *J. Chem. Phys.* **2007**, *126*, 181101.

(18) Magyar, R. J.; Tretiak, S. *J. Chem. Theory Comput.* **2007**, *3*, 976.

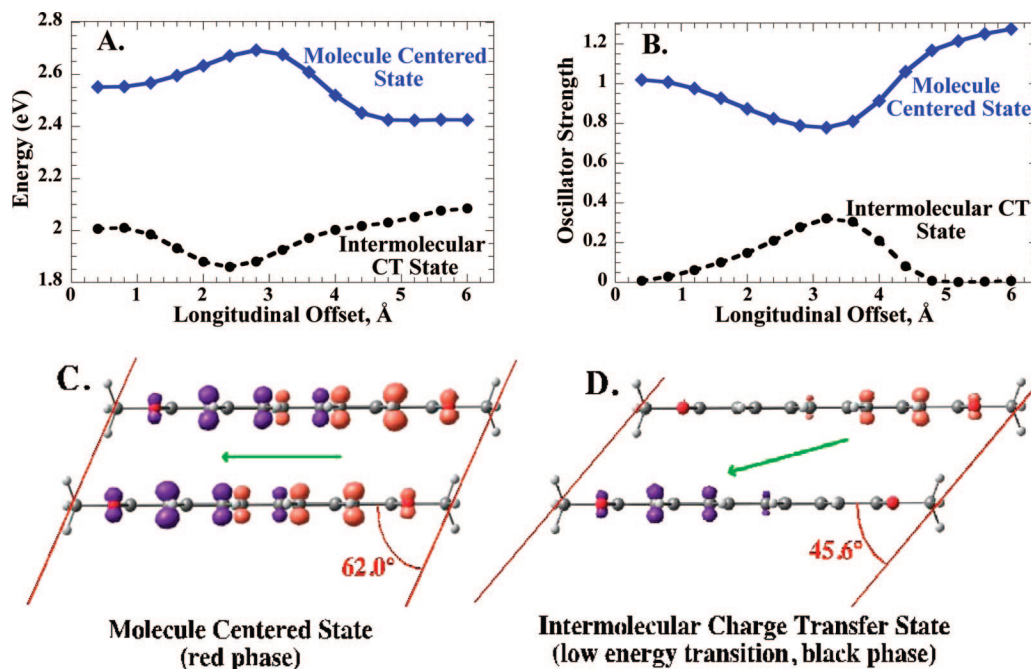


**Figure 4.** (A) Evolution of the calculated excited-state energies with longitudinal offset,  $l$ . (B) Variation of the oscillator strengths of the molecule centered state and intermolecular CT state with  $l$ . (C) Side view of molecules showing the experimentally determined tilt angle relative to the substrate and the transition density plot of the molecule centered state at  $l = 1.6$  Å. Green arrow shows the direction of transition dipole moment. Orange color: positive density. Purple color: negative density. Isodensity value: 0.0015. (D) Same as C for charge transfer state,  $l = 3.2$  Å.

chains to the electronic states of the perylene diimide,<sup>19</sup> except insofar as they determine  $t$  and  $l$ , we truncated the long side chains of PPMEEM to methyl groups in our dimer calculations. Geometry optimizations were performed at the DFT level with a B3LYP (20% Hartree–Fock exchange) exchange–correlation functional along with a 6-31G(d) split-valence polarized basis set. TD-DFT calculations were done at the same level of theory and basis set used in geometry optimizations. All geometry optimizations and excited-state calculations were performed by the Gaussian 03 program.<sup>20</sup> To test the suitability of the TD-DFT/B3LYP/6-31G(d) approach in the excited-state calculations of dimer complexes, we first compared the theoretical results with the data in a library of known perylene diimide crystal structures and absorption energies.<sup>1</sup> Here we assume an exciton in a dimer exhibits most of the photophysical behavior observed in crystals of perylene diimides. Indeed, it was shown in a number of studies that the nearest neighbor interactions

(tight-binding formalism) can be reliably used to explain the absorption and emission properties<sup>21,22</sup> (as well as the charge transport mechanisms<sup>23</sup>) in crystalline organic films and solids.

Figure 3 compares calculated lowest excited-state energies to the experimental values of compounds having various values of  $t$  and  $l$  in the crystal. There is a good correlation between the experimental data and the theoretical results. To some extent, this correlation supports the suitability of the TD-DFT/B3LYP/6-31G(d) approach to predict the optical properties of crystalline perylene diimide complexes in the solid state. Further verification of this approach will be provided later in the text where we discuss the nature of excited states involved in the absorption processes.

Transition density plots (TDs) were generated to indicate the spatial location of the excitation as well as the direction of the transition dipole moment.<sup>24</sup> These plots are particularly useful in revealing the nature of electronic transitions, for example, to distinguish between charge transfer or molecule centered (Frenkel-like) transitions. TD-DFT predicted transitions were used to construct the TDs according to eq 1,

(19) Mercadante, R.; Trsic, M.; Duff, J.; Aroca, R. *THEOCHEM (J. Mol. Struct.)* **1997**, *394* (2–3), 215.

(20) Frisch, M. J.; Trucks, G. W.; Schlegel, H. B.; Scuseria, G. E.; Robb, M. A.; Cheeseman, J. R.; Montgomery, J. A., Jr.; Vreven, T.; Kudin, K. N.; Burant, J. C.; Millam, J. M.; Iyengar, S. S.; Tomasi, J.; Barone, V.; Mennucci, B.; Cossi, M.; Scalmani, G.; Rega, N.; Petersson, G. A.; Nakatsuji, H.; Hada, M.; Ehara, M.; Toyota, K.; Fukuda, R.; Hasegawa, J.; Ishida, M.; Nakajima, T.; Honda, Y.; Kitao, O.; Nakai, H.; Klene, M.; Li, X.; Knox, J. E.; Hratchian, H. P.; Cross, J. B.; Bakken, V.; Adamo, C.; Jaramillo, J.; Gomperts, R.; Stratmann, R. E.; Yazyev, O.; Austin, A. J.; Cammi, R.; Pomelli, C.; Ochterski, J. W.; Ayala, P. Y.; Morokuma, K.; Voth, G. A.; Salvador, P.; Dannenberg, J. J.; Zakrzewski, V. G.; Dapprich, S.; Daniels, A. D.; Strain, M. C.; Farkas, O.; Malick, D. K.; Rabuck, A. D.; Raghavachari, K.; Foresman, J. B.; Ortiz, J. V.; Cui, Q.; Baboul, A. G.; Clifford, S.; Cioslowski, J.; Stefanov, B. B.; Liu, G.; Liashenko, A.; Piskorz, P.; Komaromi, I.; Martin, R. L.; Fox, D. J.; Keith, T.; AlLaham, M. A.; Peng, C. Y.; Nanayakkara, A.; Challacombe, M.; Gill, P. M. W.; Johnson, B.; Chen, W.; Wong, M. W.; Gonzalez, C.; Pople, J. A. *Gaussian 03*, Revision C.02; Gaussian, Inc.: Wallingford, CT, 2004.

(21) Chen, Z. J.; Stepanenko, V.; Dehm, V.; Prins, P.; Siebbeles, L. D. A.; Seibt, J.; Marquetand, P.; Engel, V.; Würthner, F. *Chem.–Eur. J.* **2007**, *13* (2), 436. Cornil, J.; Beljonne, D.; Calbert, J. P.; Bredas, J. L. *Adv. Mater.* **2001**, *13* (14), 1053.

(22) Seibt, J.; Marquetand, P.; Engel, V.; Chen, Z.; Dehn, V.; Würthner, F. *Chem. Phys.* **2006**, *328* (1–3), 354.

(23) Bredas, J. L.; Calbert, J. P.; daSilva, D. A.; Cornil, J. *Proc. Natl. Acad. Sci. U.S.A.* **2002**, *99* (9), 5804. Cornil, J.; Calbert, J. P.; Bredas, J. L. *J. Am. Chem. Soc.* **2001**, *123* (6), 1250. da Silva, D. A.; Kim, E. G.; Bredas, J. L. *Adv. Mater.* **2005**, *17* (8), 1072.

(24) Kose, M. E.; Mitchell, W. J.; Kopidakis, N.; Chang, C. H.; Shaheen, S. E.; Kim, K.; Rumbles, G. *J. Am. Chem. Soc.* **2007**, *129* (46), 14257. Sun, M. T. *Int. J. Quantum Chem.* **2006**, *106* (4), 1020.

$$\rho_{\mu 0}(r) = \sum_{o,u} C_{\mu o u} \varphi_o \varphi_u \quad (1)$$

where  $C_{\mu o u}$  represents the CI expansion coefficient in the basis of occupied ( $\varphi_o$ ) and unoccupied ( $\varphi_u$ ) orbitals in the electronic transition.

**Results of Calculations.** The DFT-optimized structure of PPMEEM has a planar perylene tetracarboxylic backbone with branched side chain attached to the imide nitrogens in trans configuration. TD-DFT calculation on PPMEEM predicts the lowest absorption band at 2.44 eV, 0.08 eV larger than observed experimentally in chloroform solution.

We investigate the changes in the excited states of methyl-substituted perylene diimide dimers at various longitudinal shifts where, for simplicity, the transverse shift is set to zero. For these calculations, we selected an interlayer distance of 3.45 Å, which is an average stacking distance observed in the crystals of perylene diimides substituted with different side chains.<sup>1</sup>

The evolution of excited-state energies and their corresponding oscillator strengths are given in Figure 4A,B. Calculations show two important transitions which we identify as a molecule centered state and an intermolecular CT state based on the TD plots. As an example, transition densities and the direction of the transition dipole moments are illustrated in Figure 4C,D for a longitudinal shift of 1.6 Å and 3.2 Å, respectively. There is a considerable rotation of the optical transition dipole between the CT state and the molecule centered state. Actually, the rotation of the optical transition dipole is even more pronounced than the vectors shown in Figure 4C,D. The transition dipole moment for the intermolecular charge transfer state follows a zigzag type course along the stack. Therefore, the resultant path of this transition is along the  $\pi$ - $\pi$  stacking direction.

The highest oscillator strength for the CT state (lowest for the molecule centered state) is obtained at a longitudinal shift of 3.2 Å (Figure 4B). As the energy of the CT state decreases, its oscillator strength increases. Concurrently, the energy of the molecule centered state increases and its oscillator strength decreases. The calculated oscillator strength of the CT phase may be underestimated because of the

neglect of vibronic interactions between molecules which can break-down the Born–Oppenheimer approximation yielding larger and more allowed electronic couplings.<sup>22</sup>

The calculations are in semiquantitative agreement with the experimental peak positions and absorption intensities of black and red phases shown in Figure 2 and are consistent with the more qualitative calculations of Kazmaier and Hoffmann.<sup>9</sup> The calculations also point to the intermolecular character of the CT transition that is so prominent in the observed rotation of the polarized absorbance between the red and black phases shown in Figure 1a,b.

### Summary and Conclusions

The key experimental result described here is the rotation by  $\sim 90^\circ$  of the polarized optical absorption resulting from a reversible shift in molecular stacking of only  $\sim 1.6$  Å. We assign the predominant optical transition in the red phase to a molecule centered (Frenkel) exciton. This Frenkel state remains in the black phase, but much of the oscillator strength now resides in the long wavelength intermolecular CT transition. DFT calculations support and further clarify this conclusion and demonstrate the relationship between the two optical transitions as a function of the longitudinal molecular offset. The sum of the valence and conduction bandwidths increases by  $\sim 320$  meV during this transition, a very large change for an organic semiconductor. These results show that a single material can reversibly switch between a weakly coupled molecular-like phase and a strongly coupled large bandwidth CT phase. They also demonstrate that the electrical properties of organic semiconductors are highly sensitivity to slight variations in molecular stacking and suggest that achieving optimal semiconducting properties in a device will require precise control of both crystal packing and orientation.

**Acknowledgment.** This work was funded by the U.S. Department of Energy, Office of Science, Basic Energy Sciences, Division of Chemical Sciences, Geosciences and Biosciences, under Contract No. DE-AC36-99GO10337 to NREL. CM800813H